

# Importance of AMPA Receptors for Hippocampal Synaptic Plasticity But Not for Spatial Learning

Daniel Zamanillo,<sup>1\*</sup> Rolf Sprengel,<sup>1†</sup> Øivind Hvalby,<sup>2</sup>  
 Vidar Jensen,<sup>2</sup> Nail Burnashev,<sup>1</sup> Andrei Rozov,<sup>1</sup>  
 Katharina M. M. Kaiser,<sup>1</sup> Helmut J. Köster,<sup>1</sup> Thilo Borchardt,<sup>1</sup>  
 Paul Worley,<sup>3</sup> Joachim Lübke,<sup>4</sup> Michael Frotscher,<sup>4</sup>  
 Peter H. Kelly,<sup>5</sup> Bernd Sommer,<sup>5</sup> Per Andersen,<sup>2</sup>  
 Peter H. Seeburg,<sup>1</sup> Bert Sakmann<sup>1</sup>

Gene-targeted mice lacking the L- $\alpha$ -amino-3-hydroxy-5-methylisoxazole-4-propionate (AMPA) receptor subunit GluR-A exhibited normal development, life expectancy, and fine structure of neuronal dendrites and synapses. In hippocampal CA1 pyramidal neurons, GluR-A<sup>-/-</sup> mice showed a reduction in functional AMPA receptors, with the remaining receptors preferentially targeted to synapses. Thus, the CA1 soma-patch currents were strongly reduced, but glutamatergic synaptic currents were unaltered; and evoked dendritic and spinous Ca<sup>2+</sup> transients, Ca<sup>2+</sup>-dependent gene activation, and hippocampal field potentials were as in the wild type. In adult GluR-A<sup>-/-</sup> mice, associative long-term potentiation (LTP) was absent in CA3 to CA1 synapses, but spatial learning in the water maze was not impaired. The results suggest that CA1 hippocampal LTP is controlled by the number or subunit composition of AMPA receptors and show a dichotomy between LTP in CA1 and acquisition of spatial memory.

Brief high-frequency activation of many glutamatergic pathways causes a long-lasting increase in the efficacy of synaptic transmission, termed LTP (1), and is postulated to be a model for cellular mechanisms underlying learning and memory acquisition (2). In synapses between the glutamatergic Schaffer collateral-commissural fibers of hippocampal CA3 and CA1 pyramidal cells (SC-CA1), LTP induction requires activation of the N-methyl-D-aspartate (NMDA) receptor, Ca<sup>2+</sup> influx into the postsynaptic dendritic spine, and gene activation resulting in de novo protein synthesis in the postsynaptic cell.

The hippocampus is thought to be important for spatial learning (3, 4). This has also been indicated by behavioral analysis of pharmaco-

logically treated rats (4) and genetically manipulated mice (5). However, the link between hippocampal LTP and spatial learning is controversial (6), and the pre- or postsynaptic locus of LTP expression has not been resolved (7). Yet, there is consensus that the increased synaptic efficacy characteristic of LTP is expressed as an increased AMPA receptor-mediated response to test stimuli.

AMPA receptors mediate fast excitatory postsynaptic currents (EPSCs) and for the most part are composed of two different subunits (8). In hippocampal CA1 pyramidal cells, which express mainly GluR-A and GluR-B of the four receptor subunits (9), AMPA receptors display low permeability to Ca<sup>2+</sup> due to the presence of the edited form of GluR-B in heteromeric channels (10). As a postsynaptic mechanism of LTP expression in CA1 pyramidal cells, AMPA receptors may undergo phosphorylation, perhaps at the GluR-A subunit (11). However, LTP expression may also involve insertion into the postsynaptic membrane of additional AMPA receptors (12) and may stimulate their biosynthesis (13).

## GluR-A<sup>-/-</sup> Mice and AMPA Receptor Immunocytochemistry

To study the molecular basis for LTP expression, and to probe the link between hippocampal LTP and spatial learning, we generated

mice lacking GluR-A (14) (Fig. 1, A and B). GluR-A<sup>-/-</sup> mice were smaller than their littermates during the first postnatal weeks, but after weaning their size was normal.

GluR-A gene inactivation was demonstrated by immunocytochemistry (15, 16). As shown in coronal sections (Fig. 1, C and D), the absence of GluR-A in the forebrain mostly affected AMPA receptors of the hippocampus and amygdala, where GluR-A expression is high, and had smaller effects in areas such as the neocortex, where it is normally low (17).

Immunocytochemistry (16) in the hippocampus of GluR-A<sup>-/-</sup> mice relative to wild type revealed a redistribution of the GluR-B subunit in pyramidal and dentate granule cells with increased staining over the somata (stratum pyramidale) and decreased staining in the basal (stratum oriens) and apical (stratum radiatum) dendrites (18) (Fig. 2, A and B). The altered GluR-B localization upon lack of GluR-A may indicate that the edited GluR-B subunit requires a partner for assembly or dendritic targeting of GluR-B-containing AMPA receptors. A substantial amount of GluR-B remained in the stratum lacunosum-moleculare, possibly in the form of GluR-B/C heteromeric channels, in synapses at the distalmost part of the apical dendrites of CA1 and CA3 pyramidal neurons.

Other glutamate receptor subunits (GluR-B, -C, and -D; NR1 and NR2A to C) were not up-regulated in the hippocampus of GluR-A<sup>-/-</sup> mice (shown for GluR-B, -C, and NR1 subunits in Fig. 2C).

## Distribution of Functional AMPA Receptors and Excitatory Transmission

*Glutamate-activated currents in nucleated soma-patches.* The amount of functional AMPA and NMDA receptors located in the somatic membrane of CA1 pyramidal cells was determined in nucleated soma-patches from acute brain slices (15, 19). The size of these membrane patches, which form around the nucleus, remains constant within cells of a given population, and the current amplitude elicited by glutamate application is proportional to the number of receptor channels in the patch. In wild-type mice, the mean size of currents was  $2.6 \pm 1.1$  nA (mean  $\pm$  SD;  $n = 5$ ) through nucleated CA1 soma-patches mediated by AMPA receptors at a membrane potential of  $-60$  mV and  $0.46 \pm 0.15$  nA ( $n = 5$ ) for NMDA receptors in Mg<sup>2+</sup>-free extracellular solution. In GluR-A<sup>-/-</sup> mice the AMPA receptor current was strongly reduced to  $0.12 \pm 0.13$  nA ( $n = 8$ ) (Fig. 3A), whereas the NMDA receptor current showed no significant difference with  $0.44 \pm 0.14$  nA ( $n = 8$ ;  $P = 0.76$ ;  $t$  test) (15). These results are consistent with the assumption that high GluR-A expression is a determinant of the large AMPA receptor-mediated currents in wild-type CA1 pyramidal cells.

*Evoked field excitatory postsynaptic poten-*

<sup>1</sup>Departments of Molecular Neuroscience and Cell Physiology, Max-Planck Institute for Medical Research, Jahnstrasse 29, 69120 Heidelberg, Germany.

<sup>2</sup>Department of Physiology, Institute of Basic Medical Sciences, University of Oslo, Norway. <sup>3</sup>Departments of Neuroscience and Neurology, Johns Hopkins University, School of Medicine, Baltimore MD 21205, USA. <sup>4</sup>Department of Anatomy, University of Freiburg, Albertstrasse 17, D-79104 Freiburg, Germany. <sup>5</sup>NS Research Novartis Pharma AG, Basel, Switzerland.

\*Present address: Laboratorios Doctor Esteve, Avenida Mare de Deu de Montserrat 221, 08041 Barcelona, Spain.

†To whom correspondence should be addressed. E-mail: sprengel@mpimf-heidelberg.mpg.de

## RESEARCH ARTICLES

tials (fEPSPs). Unlike the large difference in glutamate-activated AMPA currents in the soma, no differences were observed in synaptically evoked currents, as determined by fEPSP in CA1 pyramidal cell layers (19). The extracellularly recorded fEPSP had the same wave shape, and the stimulation intensity necessary to elicit equally large fEPSPs in the CA1 region was not significantly different (Fig. 3B). The mean ( $\pm$ SEM) value of the 50- $\mu$ s-long stimulation current used in slices from wild type was  $57 \pm 6 \mu\text{A}$  ( $n = 17$ ) versus  $58 \pm 9 \mu\text{A}$  ( $n = 13$ ) from GluR-A<sup>-/-</sup> mice ( $P = 0.93$ ). The corresponding fEPSP amplitudes were also similar (wild type,  $1.62 \pm 0.14 \text{ mV}$ ; GluR-A<sup>-/-</sup>,  $1.58 \pm 0.17 \text{ mV}$ ;  $P = 0.86$ ).

**Fig. 1.** GluR-A alleles and GluR-A expression in wild-type and GluR-A<sup>-/-</sup> mice. **(A)** Schematic representation of the GluR-A subunit, the GluR-A<sup>+</sup> allele, the targeted GluR-A<sup>neo</sup> allele, and the GluR-A<sup>-</sup> allele after Cre-mediated recombination (14). Black boxes represent membrane segments M1 to M4, open boxes are exonic sequences and the neo gene. LoxP sites are indicated by black triangles. Solid circles in GluR-A<sup>neo</sup> indicate 5' and 3' ends of the targeting construct. Positions of Bam HI (B) and Hind III (H) restriction sites are given. The Sac I fragment (260 bp) used as probe for the genomic blot is indicated by a black bar; P1 to P3 represent primers for screening GluR-A alleles. **(B)** Southern blot analysis of Bam HI-digested ES cell DNA visualized parts of the GluR-A<sup>+</sup>, GluR-A<sup>neo</sup>, and GluR-A<sup>-</sup> alleles as 7.2-, 9.2-, and 5.7-kb fragments, respectively. Size markers (kbp) are indicated on the left. **(C and D)** Distribution of the GluR-A subunit visualized by immunostaining in coronal forebrain sections of wild-type (C) and GluR-A<sup>-/-</sup> (D) mice (16). Cx, cortex; H, hippocampus; CP, caudate-putamen; T, thalamus; BI, basolateral amygdaloid nucleus.

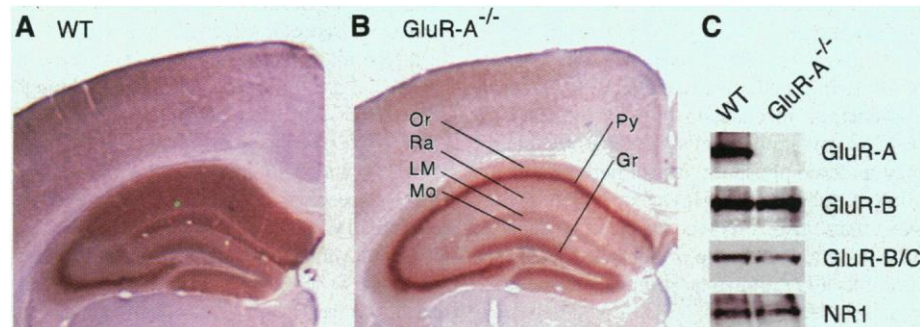
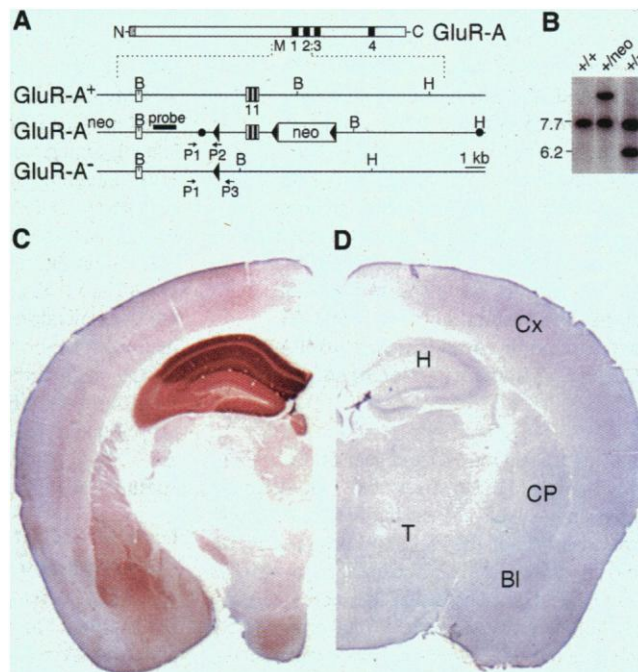


**Fig. 2.** Hippocampal expression of glutamate receptor subunits. **(A and B)** Distribution of GluR-B in somata of pyramidal cells of wild-type (A) and GluR-A<sup>-/-</sup> (B) mice in immunostainings (15) of coronal forebrain sections. Or, stratum oriens; Ra, stratum radiatum; LM, stratum lacunosum-moleculare; Mo, molecular layer; Py, stratum pyramidale; Gr, granule cell layer. **(C)** Expression of the GluR-A, -B, and -C and the NR1 subunits, monitored by immunoblots of membrane proteins from hippocampi (52) of wild-type (WT) and GluR-A<sup>-/-</sup> mice.

In SC-CA1 pyramidal cell synapses, the fEPSP was blocked in the presence of the AMPA kainate antagonist 6-cyano-7-nitroquinoxaline-2,3-dione (CNQX) (10  $\mu\text{M}$ ) (20), in slices from wild-type ( $n = 6$ ) as well as GluR-A<sup>-/-</sup> mice ( $n = 10$ ) (Fig. 3B), which demonstrates AMPA receptor-mediated neurotransmission in the absence of GluR-A.

**Miniature EPSCs (mEPSCs).** To determine directly the currents evoked by a single quantum of glutamate in individual dendritic spines of CA1 pyramidal cells, we analyzed size, time course, and peak amplitude distribution of mEPSCs (19) (Fig. 3, C and D). The average ( $\pm$ SD) peak amplitudes of mEPSCs recorded from wild-type and GluR-A<sup>-/-</sup> slices were

similar [ $12.3 \pm 1.4 \text{ pA}$  ( $n = 7$ ) and  $11.9 \pm 3.2 \text{ pA}$  ( $n = 7$ );  $P = 0.75$ ]. The decay time constant of mEPSCs in wild-type mice was monoexponential, with average time constants ranging from 4.7 to 6.1 ms in seven neurons (mean  $\pm$  SD,  $5.2 \pm 0.6 \text{ ms}$ ). In GluR-A<sup>-/-</sup> mice the monoexponential mEPSC decays were comparable ( $4.7 \pm 1.6 \text{ ms}$ ;  $n = 7$ ). In two cells, however, a small percentage (10 to 20%) of the mEPSCs had double-exponential decays with a short decay time constant of 1.5 ms and a longer one of about 12 ms. The slowly decaying component was also observed in the presence of an NMDA receptor antagonist (19). Both the short and long decay components were reversibly blocked by an AMPA receptor antagonist (19).

In summary, in spite of a strong reduction in AMPA receptor currents in the somata of CA1 pyramidal cells of GluR-A<sup>-/-</sup> mice, AMPA receptor-mediated synaptic transmission in SC-CA1 synapses appeared to be largely unaffected.

### Long- and Short-Term Changes in Hippocampal Synaptic Transmission

**LTP.** We examined LTP in CA1 in slices from adult mice. In wild-type mice, tetanic stimulation of the afferent fibers, in either stratum radiatum or stratum oriens, produced a persistent homosynaptic potentiation of the synaptic responses, characteristic of LTP (3, 21). The average fEPSP slope 40 to 45 min after tetanization was  $135\% \pm 9\%$  (mean  $\pm$  SEM;  $n = 17$ ; four mice) of the pretetanic control value and synaptic transmission in the control pathway was unchanged ( $100\% \pm 2\%$ ). In GluR-A<sup>-/-</sup> mice, however, the tetanized pathway was not significantly different from the control pathway ( $109\% \pm 6\%$  versus  $104\% \pm 5\%$ ;  $n = 13$ ; five mice;  $P = 0.27$ ) (Fig. 4A). Lack of LTP was not due to inefficient tetanization because the first fEPSP and the summed voltage integral of the high-frequency trains used to elicit LTP were not significantly different in wild-type and GluR-A<sup>-/-</sup> mice ( $P = 0.45$  and  $P = 0.09$ ), which is consistent with the normal excitatory transmission in the mutant animals.

Induction of LTP is facilitated by  $\gamma$ -aminobutyric acid type A (GABA<sub>A</sub>) receptor blockade, whereas the magnitude of LTP is unchanged (22). Thus, we added bicuculline (10  $\mu\text{M}$ ) to ensure that the lack of LTP in GluR-A<sup>-/-</sup> mice was not due to an induction failure. To reduce the resulting hyperexcitability, we cut between the CA3 and CA1 areas and raised both  $\text{Ca}^{2+}$  and  $\text{Mg}^{2+}$  to 4 mM, which yielded a similar amount of LTP ( $134\% \pm 4\%$ ;  $n = 9$ ; four mice;  $P = 0.90$ ). In the presence of bicuculline, LTP in slices from wild-type mice measured  $140\% \pm 6\%$  (control pathway,  $100\% \pm 2\%$ ) ( $n = 17$ ; five mice), whereas LTP was absent in GluR-A<sup>-/-</sup> mice (tetanized versus control pathway:  $100\% \pm 5\%$  versus  $99 \pm 3\%$ ;  $n = 20$ ; six mice;  $P = 0.93$ ) (Fig. 4B). To

ensure that the tetanization paradigm gave robust and long-lasting LTP, we sometimes followed responses in wild-type slices for 4 or 8 hours. The measured fEPSP slope relative to the pretetanic value was  $168\% \pm 23\%$  ( $n = 6$ ) after 4 hours and  $160\% \pm 8\%$  ( $n = 2$ ) after 8 hours.

**Paired-pulse facilitation.** CA1 excitatory synapses show paired-pulse facilitation (23),

a form of short-term presynaptic plasticity (24) that decays within a few hundred milliseconds. The facilitation in slices from wild-type and *GluR-A*<sup>-/-</sup> mice, tested at three interstimulus intervals (Fig. 4C), was not significantly different (25). Hence, the failure to generate LTP in SC-CA1 connections suggests that there is a postsynaptic deficiency in *GluR-A*<sup>-/-</sup> animals.

**Hippocampal CA1 Pyramidal Cell Dendrites and Spines**

**Structure of excitatory synapses.** The vast majority of synapses in stratum radiatum of CA1 are formed by collaterals of ipsilateral and contralateral CA3 pyramidal cell axons. These glutamatergic terminals form asymmetric contacts on dendritic spines (Fig. 5, A and B) and shafts (Fig. 5, C and D) of CA1 pyramidal neurons. Electron microscopic analysis (26) of more than 100 spine and shaft synapses in both wild-type and *GluR-A*<sup>-/-</sup> mice did not reveal differences between the two groups. At the light microscopic level, we evaluated the total number of dendritic spines, spine density, and spine distribution on main apical dendrites of identified, Golgi-impregnated CA1 pyramidal cells. We found no significant differences in spine density between wild-type ( $1.71 \pm 0.14$  spines per micrometer) and *GluR-A*<sup>-/-</sup> ( $1.73 \pm 0.14$ ;  $P = 0.34$ ) mice.

**Dendritic calcium transients.** We next measured dendritic Ca<sup>2+</sup> transients (27) as an indicator of stimulus-evoked postsynaptic membrane depolarization (Fig. 6, A and B). Dendritic resting Ca<sup>2+</sup> concentrations were  $167 \pm 83$  nM (mean  $\pm$  SD;  $n = 4$ ) for wild-type and  $149 \pm 93$  nM ( $n = 7$ ) for *GluR-A*<sup>-/-</sup> mice. During tetanic stimulation, the dendritic Ca<sup>2+</sup> transients evoked by a single stimulus accumulated to reach a steady-state plateau, which was similar ( $P = 0.73$ ) in wild-type ( $690 \pm 193$  nM;  $n = 4$ ) and *GluR-A*<sup>-/-</sup> ( $624 \pm 343$  nM;  $n = 7$ ) mice. This, together with the comparable stimulus intensities, indicated that dendritic AMPA receptor-mediated membrane depolarization during tetanic stimulation and postsynaptic Ca<sup>2+</sup> entry were unaffected in *GluR-A*<sup>-/-</sup> mice.

**Spinous calcium transients.** We analyzed spinous Ca<sup>2+</sup> transients (27) mediated by NMDA receptors in hippocampal spines to determine whether induction of the signal cascade for LTP is functional (Fig. 6, C and D). In wild-type slices the EPSP-evoked Ca<sup>2+</sup> transients in single spines generated a fluorescence amplitude,  $\Delta F/F_{max}$ , of  $0.40 \pm 0.13$  (mean  $\pm$  SD;  $n = 8$ ), similar to that in *GluR-A*<sup>-/-</sup> mice ( $0.44 \pm 0.16$ ;  $n = 8$ ;  $P = 0.49$ ). The fluorescence change in the parent dendritic shaft during an evoked EPSP was  $<30\%$  of the amplitude recorded in the spine ( $n = 5$ ) in both genotypes. D(-)-2-Amino-5-phosphonopenta-

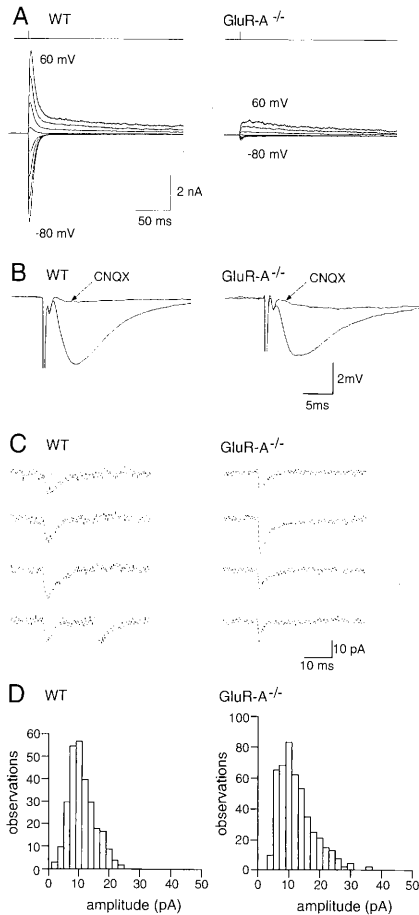


**Fig. 3.** Glutamate-activated somatic and synaptic currents in CA1 pyramidal cells of wild-type (WT) and *GluR-A*<sup>-/-</sup> mice. (A) Currents in nucleated soma-patches activated by brief pulses (2 ms) of glutamate (1 mM), indicated by upward deflection in the trace above the current records, applied to nucleated soma-patches of CA1 pyramidal neurons at membrane potentials ranging in 20-mV steps from -80 to 60 mV in extracellular physiological solution with 1 mM MgCl<sub>2</sub> (19). (B) fEPSP recorded in stratum radiatum of the CA1 region of brain slices after extracellular SC stimulation before and after addition of CNQX (10  $\mu$ M) (19). Stimulus intensities were 40  $\mu$ A (wild type) and 25  $\mu$ A (*GluR-A*<sup>-/-</sup>). The stimulus artifact has been truncated. (C) mEPSCs recorded from individual CA1 pyramidal cells in slices at -70 mV holding potential and 23°C (19). (D) Peak amplitude distribution of mEPSCs from experiments as shown in (C). Distribution was similar for both genotypes and typically showed a tail of larger amplitudes. Mean peak amplitude was  $12.4 \pm 5.0$  pA ( $n = 290$ ) in wild-type and  $14.4 \pm 7.1$  pA ( $n = 495$ ) in *GluR-A*<sup>-/-</sup> mice. Observations and mEPSCs were recorded from one cell.

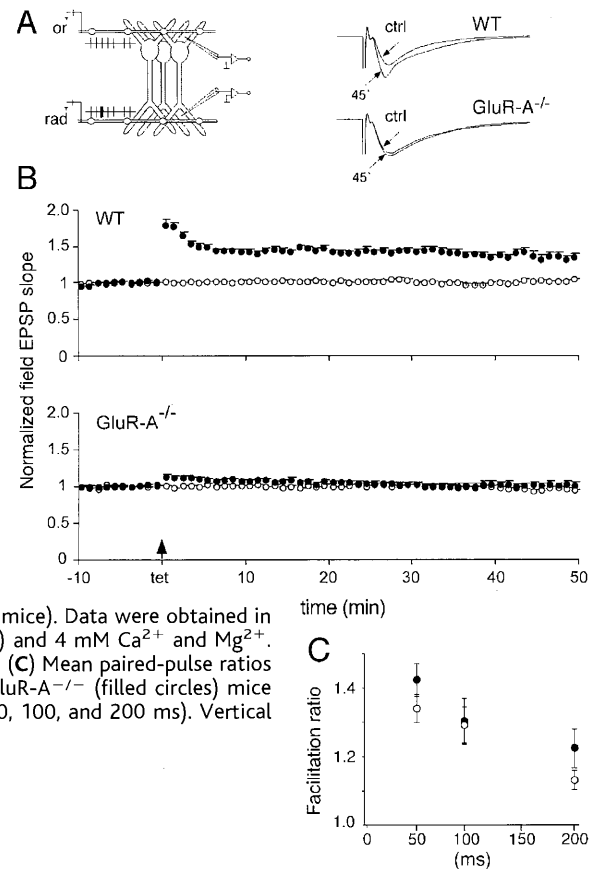


**Fig. 4.** Synaptic plasticity in the hippocampal CA1 region. (A) (Left) Diagram of electrode arrangement. Stimulation electrodes placed in stratum radiatum (rad) and stratum oriens (or). Synaptic field responses were monitored by two extracellular recording electrodes placed in the corresponding synaptic layers. (Right) Extracellular recording of fEPSPs in slices before and after tetanization. The two pairs of traces show superimposed averages of 10 consecutive field responses from the tetanized pathway before (ctrl) and 45 min after LTP induction (45') in a wild-type (WT) and a *GluR-A*<sup>-/-</sup> slice. (B) Summary graphs of extracellular fEPSP slopes evoked in the tetanized (filled circles) and untetanized (open circles) pathways from slices of wild-type (WT;  $n = 17$ ; five mice) and *GluR-A*<sup>-/-</sup> ( $n = 20$ ; six mice). Data were obtained in bicuculline methochloride (10  $\mu$ M) and 4 mM Ca<sup>2+</sup> and Mg<sup>2+</sup>. Arrow, time of tetanic stimulation. (C) Mean paired-pulse ratios for wild-type (open circles) and *GluR-A*<sup>-/-</sup> (filled circles) mice at three interstimulus intervals (50, 100, and 200 ms). Vertical bars indicate SEM.

noic acid (AP-5) (50  $\mu$ M) in the extracellular solution reduced  $Ca^{2+}$  transients to 12% in wild-type and 14% in GluR-A<sup>-/-</sup> mice ( $n = 2$  each), which suggests that the NMDA receptor-mediated  $Ca^{2+}$  entry into CA1 pyramidal cells is not altered in the mutant.

**Immediate-early gene (IEG) expression.** We compared wild-type and GluR-A<sup>-/-</sup> mice for IEG expression, acutely up-regulated after a maximal electroconvulsive shock (MECS) (28, 29). The induction, which largely depends on NMDA receptors, of *c-fos*, *c-jun*, *zif268*, and *RGS2*, and the cellular expression patterns did not differ in the two genotypes, as determined by in situ hybridization in brain sections (28). We conclude that the link between physiological synaptic activity and activity-dependent gene expression is preserved in GluR-A<sup>-/-</sup> mice.

### Spatial Learning

Given the strong effect of GluR-A deficiency on hippocampal CA1 LTP, one might expect deficits in the water maze test (2, 6). However, spatial learning of GluR-A<sup>-/-</sup> mice was not significantly different from that of wild-type mice (30). In both groups, the latency between start of swimming and finding the hidden platform decreased from about 60 to 20 s after about 5 days of training (Fig. 7A). There were no differences between groups in latency or distance swum before they found the platform

(analysis of variance,  $P = 0.26$  and  $0.52$ , respectively) and no group-trial block interactions ( $P = 0.15$  and  $0.07$ , respectively), but trial block effects were highly significant ( $P < 0.001$  for both). The slightly increased latency in GluR-A<sup>-/-</sup> mice during the first training trials can be explained by the reduced swimming performance of GluR-A<sup>-/-</sup> mice compared with wild type (Fig. 7B). Spatial memory acquisition was further compared by a transfer test, with the platform removed from the pool after 10 blocks of trials. Both wild-type and GluR-A<sup>-/-</sup> mice spent most of 60 s in the SE quadrant, which previously contained the platform (Fig. 7C), with no significant difference between genotypes ( $P = 0.19$ ). The groups also did not differ in the number of times they crossed the annulus representing the platform position (mean  $\pm$  SEM: wild-type,  $5.4 \pm 0.7$ ; GluR-A<sup>-/-</sup>,  $5.5 \pm 0.9$ ;  $P = 0.98$ ).

When we performed the transfer test without visual cues, there was no quadrant preference (Fig. 7D). In neither group did the time spent in the target quadrant differ from chance ( $P > 0.25$ ) and the groups did not differ ( $P = 0.65$ ) in this measure.

### Discussion

There are three main observations: (i) in spite of the severe loss of AMPA receptors in soma-patches of CA1 cells, excitatory synaptic transmission appeared normal in GluR-

A<sup>-/-</sup> mice; (ii) although synaptic transmission was normal, NMDA receptor-mediated LTP was lacking in CA1 pyramidal neurons; (iii) despite the lack of SC-CA1 LTP, spatial learning was normal.

**Normal excitatory synaptic transmission.** GluR-A deficiency underlies the selective loss of extrasynaptic AMPA receptors in CA1 pyramidal cells. This is demonstrated by the strong reduction of AMPA receptor-mediated currents in soma-patches versus the normal responses at CA1 dendritic synapses, as shown by mEPSCs with regular amplitude range and rise times and fEPSP in response to radiatum fiber activation. It might suggest that, in wild-type mice, GluR-A-containing receptors do not contribute to synaptic transmission and that synaptic transmission is carried by GluR-B/C and GluR-B/D AMPA receptor subtypes, which are not affected in GluR-A<sup>-/-</sup> mice. This is unlikely because high-resolution immunocytochemistry indicates that GluR-A-containing receptors are located in synapses (31). Moreover, the additional slow component occasionally observed in mEPSC decay in the mutant might indicate a change in synaptic AMPA receptor subtypes. Therefore, we think that, after a strong reduction in the total number of AMPA receptors in GluR-A<sup>-/-</sup> CA1 cells, the remaining GluR-B/C and GluR-B/D receptors are preferentially transported and targeted to synapses and substitute for the missing GluR-A/B subtype. There are not enough AMPA receptors left for extrasynaptic sites.

This preference of dendritic over somatic membrane insertion, revealed by GluR-A<sup>-/-</sup> mice, also may explain why, in certain neuronal cell populations such as cerebellar granule cells, synaptic AMPA receptor currents are prominent even though the soma-patch currents are very low (32). In such neuronal populations AMPA receptor expression is lower than in CA1 pyramidal cells and thus, as in CA1 cells of GluR-A<sup>-/-</sup> mice, the number of available receptors might not suffice to occupy extrasynaptic sites.

An intriguing consequence of GluR-A deficiency is the intracellular redistribution of the GluR-B subunit, which, in the mutant, becomes largely restricted to the soma of hippocampal pyramidal and dentate granule cells, where it may reside in the endoplasmic reticulum or Golgi apparatus. Explanations for this redistribution could be that GluR-B homomeric channels do not form efficiently or that GluR-B homomers do not reach synapses. Hence, we postulate that, in GluR-A<sup>-/-</sup> CA1 neurons, a major fraction of GluR-B has no partner subunit for heteromeric AMPA receptor assembly.

**Lack of hippocampal SC-CA1 LTP.** The observation that the dendritic and spinous  $Ca^{2+}$  transients are not different between wild-type and GluR-A<sup>-/-</sup> mice shows that the initial steps of the induction mechanism

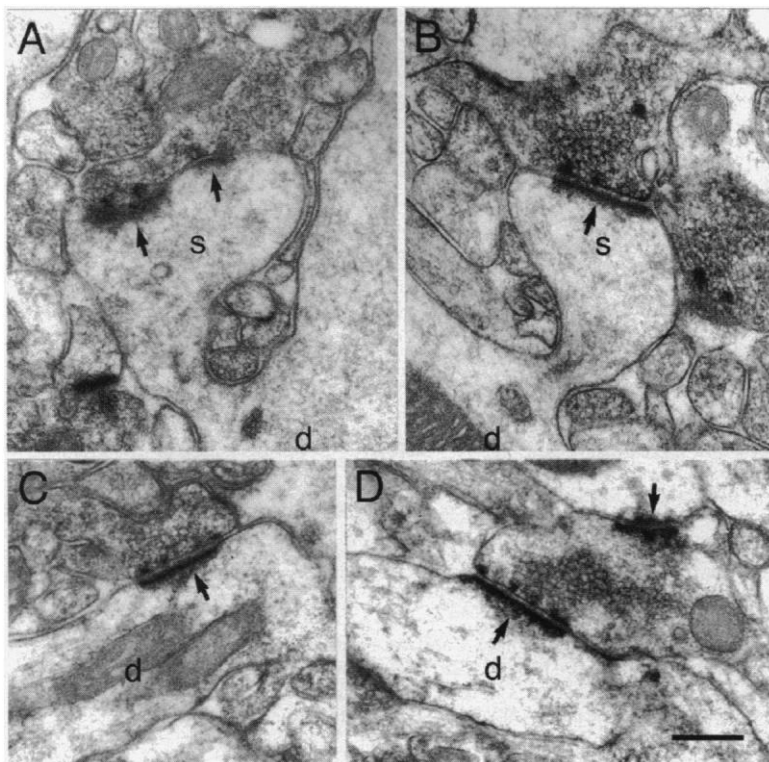


**Fig. 5.** Synaptic contacts on pyramidal cell dendrites in CA1 stratum radiatum. Representative, supposedly glutamatergic, asymmetric axospinous synaptic contacts (arrows) formed on dendritic spines (s) arising from dendritic shafts (d). Morphologically, synaptic contacts in wild-type (A) and GluR-A<sup>-/-</sup> (B) mice were indistinguishable. (C and D) Axodendritic synaptic contacts in wild-type (C) and GluR-A<sup>-/-</sup> (D) mice were indistinguishable. Bar = 0.25  $\mu$ m.

## RESEARCH ARTICLES

of LTP, which depend on NMDA receptor and voltage-dependent calcium-channel activation, are unaltered. In  $\text{GluR-A}^{-/-}$  mice,  $\text{Ca}^{2+}$ -dependent cellular signaling cascades can be activated, and IEG responses in MECS-treated  $\text{GluR-A}^{-/-}$  mice are the same as in wild type. Thus, the expression of LTP is likely to be blocked in the mutant.

LTP expression is manifested by an increased fEPSP amplitude and probably reflects a modification of the molecular structure of the postsynapse. The enhanced AMPA receptor-mediated response to presynaptically released glutamate could depend on the number or the subunit composition of functional AMPA

receptors in the subsynaptic membrane. In  $\text{GluR-A}^{-/-}$  mice LTP expression could be compromised in several ways.

CA1 neurons of wild-type mice may contain excess  $\text{GluR-A}$ -containing AMPA receptors, which are essential for rapid incorporation of additional AMPA receptors into the postsynaptic membrane after tetanization. Because of the lack of  $\text{GluR-A}$ , and hence of spare AMPA receptors (33), this postulated step in LTP expression would be deficient in  $\text{GluR-A}^{-/-}$  mice. Alternatively, LTP expression may require AMPA receptor subunit modification. One hypothesis is that the signaling cascade initiated by  $\text{Ca}^{2+}$  influx during tetanization

might be linked to phosphorylation of AMPA receptors, preferentially via the  $\text{GluR-A}$  subunit (11). In the absence of this subunit, AMPA receptor phosphorylation would be expected to be strongly reduced. This study cannot distinguish between these alternatives, although the residual LTP in the dentate gyrus of  $\text{GluR-A}^{-/-}$  mice (34) argues against a general requirement for  $\text{GluR-A}$  in LTP expression.

*Normal spatial learning in the absence of SC-CA1 LTP.* This finding adds to a growing number of examples of a dichotomy between LTP and learning (6, 35). One explanation could be that mice may use extrahippocampal structures to solve the Morris water maze. It is possible that LTP, although not critical for the type of reference memory test used here, could be important in spatial tasks that involve only episodic or working memory (36). Alternatively, learning is associated with LTP at a degree of synaptic involvement that is too small to be detected with conventional electrophysiological field recordings. Furthermore, the spatial task might not require LTP in SC-CA1 synapses.

Notably, a genetically engineered CA1 NMDA receptor deficiency had also generated LTP deficiency, but learning in the water maze was impaired (5). One explanation for the dif-

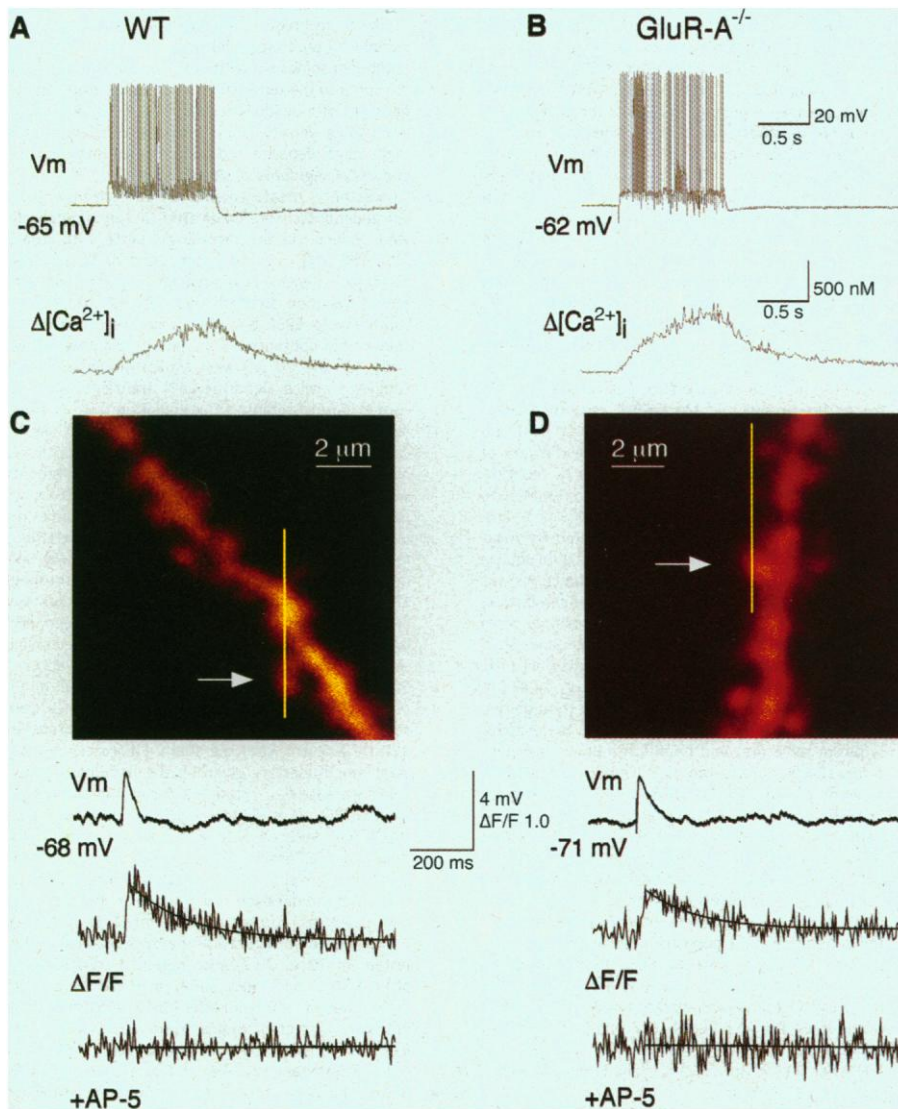


**Fig. 6.** Dendritic (A and B) and spinous (C and D)  $\text{Ca}^{2+}$  transients in CA1 pyramidal cells during synaptic stimulation. (A and B) (Upper traces) Somatic recorded action potentials evoked by tetanic stimulation of SC in CA1 pyramidal neuron in a slice of wild-type (WT) (A) and  $\text{GluR-A}^{-/-}$  (B) mouse. (Lower traces) Corresponding dendritic  $\text{Ca}^{2+}$  signal measured simultaneously in the same neuron. (C and D) Images of an apical oblique dendritic branch and spines of a CA1 pyramidal cell in a slice from wild-type (C) and  $\text{GluR-A}^{-/-}$  (D) mouse. Lines indicate positions of line scans for fluorescence recording of individual spines (arrows). (Upper traces) Somatic recording of a single EPSP evoked by focal extracellular stimulation of SC nerve terminals synapsing on a CA1 pyramidal cell. (Middle traces) EPSP-evoked  $\text{Ca}^{2+}$  fluorescence transient recorded in a single active dendritic spine shown in the image above. (Lower traces) Fluorescence record after addition of  $50 \mu\text{M}$  AP-5.

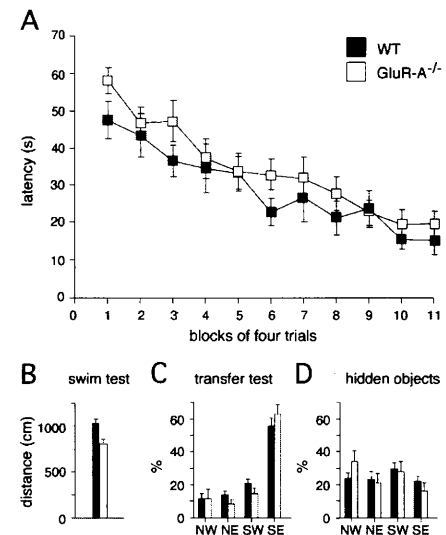


**Fig. 7.** Spatial learning. (A) In a Morris water maze the mean latency ( $\pm$  SEM) to escape from the pool to the submerged platform (eight trials per day in blocks of four) is presented as a function of trial block for male wild-type ( $n = 19$ ) (filled squares) and  $\text{GluR-A}^{-/-}$  ( $n = 21$ ) (open squares) mice. (B) Swim test gives the mean distance covered by the two genotypes in 50 s in the pool without a platform before training. (C) In a transfer test after trial block 10, the platform was removed and wild-type and  $\text{GluR-A}^{-/-}$  mice were allowed to search for 60 s. Both groups searched selectively in the target quadrant (SE). Ordinate, percent time spent in each quadrant. (D) Quadrant preference was not observed when distal visual cues were invisible in the transfer test.

ference in learning might be that the induction phase of LTP is impaired in the NMDA receptor but not in the AMPA receptor mutant. During this phase the spinous  $Ca^{2+}$  transients affect numerous signaling pathways, which might be essential for memory acquisition. In this context, it might be asked how the fEPSP LTP phenomenon is related to normal physiology in the hippocampus. The highly synchronous ensemble activity of CA3 pyramidal neurons required to induce standard fEPSP-LTP may not normally occur.

In summary, adult hippocampal LTP depends on the number and subunit composition of AMPA receptors. Therefore, in adult animals, LTP appears to be essentially a postsynaptic mechanism. However, this particular form of synapse modifiability in CA1 is not required for a reference memory test.

### References and Notes

1. T. V. Bliss and T. Lomo, *J. Physiol. (London)* **232**, 331 (1973).
2. D. V. Madison, R. C. Malenka, R. A. Nicoll, *Annu. Rev. Neurosci.* **14**, 379 (1991); T. V. Bliss and G. L. Collingridge, *Nature* **361**, 31 (1993).
3. P. Andersen, *Prog. Brain Res.* **58**, 419 (1983).
4. R. G. Morris et al., *Nature* **319**, 774 (1986).
5. J. Z. Tsien, P. T. Huerta, S. Tonegawa, *Cell* **87**, 1327 (1996).
6. D. M. Bannerman et al., *Nature* **378**, 182 (1995); K. J. Jeffery, *Hippocampus* **7**, 95 (1997).
7. D. M. Kullmann and S. A. Siegelbaum, *Neuron* **15**, 997 (1995).
8. R. J. Wenthold et al., *J. Neurosci.* **16**, 1982 (1996).
9. K. Keinänen et al., *Science* **249**, 556 (1990); J. Boulter et al., *ibid.*, p. 1033.
10. N. Burnashev et al., *Neuron* **8**, 189 (1992); M. Hollmann, M. Hartley, S. Heinemann, *Science* **252**, 943 (1991); R. I. Hume et al., *ibid.* **253**, 1028 (1991).
11. A. Barria et al., *Science* **276**, 2042 (1997); K. W. Roche et al., *Neuron* **16**, 1179 (1996).
12. P.-M. Lledo et al., *Science* **279**, 399 (1998).
13. A. Nayak et al., *Nature* **394**, 680 (1998).
14. The targeting vector pFC II contained 10.7 kb of the murine GluR-A gene (*GRIA1*) with parts of introns 10 and 11 and exon 11, numbered according to the GluR-B gene (37). The *neo* selection marker (ploxneo3) (38) was inserted into an Eco NI site, 700 base pairs (bp) into intron 11. In addition, 225 nucleotides upstream of exon 10, a 28-bp Pfl MI fragment was substituted by a 34-bp loxP site. Embryonic stem (ES) cells (R1) (39) were electroporated with the targeting vector and linearized at the unique Hind III site in the polylinker, and five positive clones were identified by polymerase chain reaction (PCR) with primers P1 (5' TCTCATTGTGATGACCCATCC 3') and P2 (5' CTGCCATGAATAATACTTCG 3') and confirmed by Southern blotting (Fig. 1B) with a 162-bp Sac I fragment of intron 10 as 5' outside probe. ES cell clone 12.5 was transfected with an expression vector for Cre recombinase (pMC-Cre) (40), and clones with one remaining loxP site were identified by PCR with primers P1 and P3 (5' CTGCCTGGGTAAGTGAAGTGG 3') (Fig. 1A). Subclone 36.5 was injected into C57BL6 blastocysts, chimeric animals were backcrossed to C57BL6, and intercrosses produced 25% GluR-A<sup>-/-</sup> mice.
15. For all analyses we used littermates of F<sub>2</sub> and F<sub>3</sub> backcrosses to C57BL6. Electrophysiological analyses were restricted to animals between P42 and P45. For the anatomical and behavioral analyses mice were 2 to 3 months old. LTP measurements were performed on mice at 3 months of age. To preclude bias, the experimenters of the LTP, anatomical, and behavioral measurements were blind with respect to the genotype of the mice analyzed. All data were statistically evaluated by two-tailed *t* tests.
16. Vibratome-cut sections (50 μm) were incubated for 15 min in phosphate-buffered saline (PBS) containing 50% methanol and 30% H<sub>2</sub>O<sub>2</sub>, washed with PBST (PBS containing 0.2% Triton X-100), blocked for 30 min with PBST containing 5% normal goat serum (NGS), and preincubated for 30 min at room temperature (RT) in 4% NGS containing 0.4% Triton X-100. Sections were kept overnight at 4°C in 2% NGS containing 0.4% Triton X-100 with glutamate receptor 1 polyclonal antibody at 1 to 3 μg/ml (Chemicon, Temecula, CA) and glutamate receptor 2 polyclonal antibody at 5 μg/ml (Pharmingen, San Diego, CA). Sections were rinsed repeatedly with PBST and incubated for 30 min in PBST containing a 1:200 dilution of biotinylated secondary antibody (Vector Laboratories). Sections were washed with PBST, incubated for 30 min in PBST containing horseradish peroxidase-avidin-biotin complex (1:50) (Vectastain ABC Elite Kit, Vector Laboratories), washed with PBST, washed with PBS, and developed for peroxidase activity in 0.05% 3,3'-diaminobenzidine hydrochloride (Sigma) containing 0.01% peroxide. After a brief rinse in PBS, sections were mounted to glass slides, dried overnight at RT, dipped into xylol, and coverslipped in Vitro-Clud (R. Langenbrinck, Emmerdingen).
17. E. Molnár et al., *Neuroscience* **53**, 307 (1993).
18. R. S. Petralia et al., *J. Comp. Neurol.* **385**, 456 (1997).
19. Brain slices were prepared (41) and recordings from nucleated patches (42) isolated from the soma of CA1 pyramidal neurons were done with pipettes of 5 to 7 MΩ access resistance. On average, one to three cells per mouse were analyzed. The NMDA and AMPA receptor-mediated currents were measured in nominally Mg<sup>2+</sup>-free extracellular solution in the presence of 2,3-dioxo-6-nitro-1,2,3,4-tetrahydrobenzo-[f]quinoxaline-7-sulfonamide (5 μM) and AP-5 (50 μM), respectively. Membrane potentials were clamped to values changing stepwise from -80 to 60 mV. Soma-patch currents were evoked by brief (2 ms) application of glutamate (1 mM). mEPSCs were recorded from slices (one slice per mouse) at -70 mV in the presence of the GABA<sub>A</sub> receptor blocker bicuculline (20 μM) and tetrodotoxin (1 μM) and analyzed as described (43). To enhance the rate of mEPSCs, we increased the extracellular K<sup>+</sup> concentration in some experiments from 2.5 to 5 mM (2 to 10 min). Only mEPSCs with a 20 to 80% peak amplitude rise time of ≤1 ms were selected for measurements of peak amplitude and decay time course. A single or the sum of two exponential functions was fitted to the mEPSC decay by SIMPLEX minimization. fEPSPs were recorded in CA1 of hippocampal slices prepared from mice sacrificed with halothane. Brain slices were maintained in an interface chamber (44). Orthodromic synaptic stimulation (50 μs, <119 μA, 0.2 Hz) in CA1 was delivered alternately through two tungsten electrodes to activate synapses in the apical (stratum radiatum) and basal (stratum oriens) dendrites. Extracellular potentials were monitored by similarly placed glass electrodes filled with extracellular solution. After stable synaptic responses in both pathways for at least 15 min, one pathway was tetanized (100 Hz, 1 s), and the other served as a control. To standardize the tetanization strength, we set the tetanic stimulation strength in response to a single shock at an intensity just above the threshold for generation of a population spike. We assessed synaptic efficacy by measuring the slope of the fEPSP in the middle third of its rising phase. Six consecutive responses (1 min) were averaged and normalized to the mean value recorded 4 to 7 min before tetanic stimulation.
20. J. F. Blake, M. W. Brown, G. L. Collingridge, *Neurosci. Lett.* **89**, 182 (1988).
21. P. Andersen et al., *Nature* **266**, 736 (1977).
22. H. Wigström and B. Gustafsson, *ibid.* **301**, 603 (1983); H. Wigström and B. Gustafsson, *Acta Physiol. Scand.* **125**, 159 (1985).
23. P. Andersen, *Acta Physiol. Scand.* **48**, 178 (1960).
24. B. Katz and R. Miledi, *J. Physiol. (London)* **195**, 481 (1968).
25. At pulse intervals of 50, 100, and 200 ms, the facilitation ratios (mean ± SEM) were 1.42 ± 0.05 (*n* = 16), 1.30 ± 0.07 (*n* = 10), and 1.22 ± 0.06 (*n* = 10) in wild-type and 1.34 ± 0.04 (*n* = 18), 1.29 ± 0.05 (*n* = 12), and 1.13 ± 0.03 (*n* = 12) in GluR-A<sup>-/-</sup> mice. Ratios were calculated from experiments in which the second facilitated response was just below threshold for eliciting a population spike. The ratios in the two groups were not significantly different (*P* = 0.17, 0.90, and 0.12, respectively).
26. Animals were anesthetized with sodium pentobarbital (50 mg/kg) and perfused transcardially with 0.9% NaCl followed by a fixative containing 1% paraformaldehyde, 2.5% glutaraldehyde, and 0.1% picric acid in 0.1 M phosphate buffer (pH 7.4). After post-fixation of the brain overnight (4°C), we processed vibratome sections (100 μm) for electron microscopy (45). Ultrathin sections were cut on a Reichert Ultratuc microtome, stained with uranyl acetate and lead citrate, and examined in a Philips CM 100 electron microscope. In addition to regular electron microscopy of spine and shaft synapses in stratum radiatum of the CA1 region, the total number and density of spines on apical dendrites of identified CA1 pyramidal cells were quantified in two wild-type and two GluR-A<sup>-/-</sup> mice. Golgi impregnation of vibratome sections (150 μm) was carried out by the sandwich technique (46). We stained randomly selected CA1 pyramidal neurons and counted the total number of spines along the main apical dendrite from the soma to the terminal bifurcation in camera lucida drawings of individual dendrites (*n* = 10). We calculated spine density (spines per micrometer) for the main apical dendrite and for proximal, intermediate, and distal segments of equal length.
27. Fluorescence measurements of Ca<sup>2+</sup> transients in apical dendrites were made after CA1 pyramidal cells were loaded via the recording pipette with fura-2 (250 μM) (47). Cells were stimulated via SC inputs at 50 Hz for 1 s with an extracellular tungsten electrode. The stimulation strength was first set to evoke a subthreshold EPSP and then increased to evoke a single action potential. Stimulation parameters (typically 180 μA, 70 μs) were similar in wild-type and GluR-A<sup>-/-</sup> mice. Dendritic Ca<sup>2+</sup> transients were recorded during tetanic SC stimulation with a back-illuminated frame transfer charge-coupled device camera with a 10-ms time resolution. Dendritic regions of interest for fluorescence measurements were located on the main apical dendrite 26 ± 15 μm (mean ± SD; *n* = 11) distal to the soma. We used the standard ratioing equation to convert fluorescence transients to Ca<sup>2+</sup> concentrations (48). Spinous Ca<sup>2+</sup> transients evoked by single subthreshold EPSPs were recorded with multiphoton microscopy (49) using the Ca<sup>2+</sup> indicator Oregon Green 488 BAPTA-1 (200 μM). Fluorescence was recorded in line scan mode. We evoked EPSPs by focal stimulation of SC afferents with an extracellular pipette with its tip placed close (<10 μm) to the dendrite. Spines were selected on secondary or tertiary dendritic branches 100 to 300 μm from the soma. Fluorescence transient amplitudes are given by the maximal fluorescence increase  $F_{max}$  relative to basal fluorescence  $F_0$ , as in  $(\Delta F/F)_{max} = (F_{max} - F_0)/(F_0 - \text{background})$ .
28. MECS was induced with a constant current signal generator (ECT Unit, UGO Basile) connected by non-traumatic ear clips. The signal parameters were as follows: pulse duration, 1 s; frequency, 100 Hz; pulse width, 0.3 ms; current, 17 mA. MECS produced an immediate tonic seizure with hindlimb extension that lasted for 10 to 20 s. Mice regained consciousness after 1 to 2 min. Mice were sacrificed by cervical dislocation 75 to 90 min after MECS, and brains were promptly dissected. Brains from unstimulated and from MECS-stimulated wild-type and GluR-A<sup>-/-</sup> mice were frozen together in Tissue-Tek (Sakura Finetek) and were blocked and sectioned together for better comparison. Horizontal sections (20 μm), which included cingulate, sensory, motor, and pyriform cortical regions; amygdala; dentate gyrus; CA1-4; and subiculum were prepared on a cryostat (Miccrom) and processed for in situ hybridization with <sup>35</sup>S-labeled RNA probes (50).
29. P. F. Worley et al., *Cold Spring Harbor Symp. Quant. Biol.* **55**, 213 (1990).
30. Morris water maze: The pool was 133 cm in diameter with white interiors and 60-cm-high walls and it rested on a 40-cm pedestal. The platform was 8 × 8 cm, with the top surface painted white and covered

with wire mesh (8 mm between wires), and 42 cm high. The water level was 1.6 cm above the level of the platform, which was placed in the middle of one quadrant (SE) of the pool, midway between wall and pool center. The water ( $21^{\circ} \pm 2^{\circ}\text{C}$ ) was made opaque by the addition of 7.2 kg of powdered low-fat milk. Tracking of mice was as described (57). A month before the actual experiment, the mice swam daily for 13 days (platform NW) in a smaller pool (60 cm), which accustomed them to mounting the platform. **Spatial navigation trials:** Mice (19 wild type, 21 GluR-A<sup>-/-</sup>) were gently placed into the water at the edge of the pool at one of four start positions arbitrarily named N, S, E, and W. In a block of four trials all start positions were used in a semirandom order that differed every day. Finding the platform was defined as climbing onto it and staying for at least 5 s. Once on the platform, the mouse was allowed to stay for 30 s. For any mouse that failed to find the platform within 90 s, a latency of 90 s was recorded, and the mouse was placed on the platform. To ensure that the mouse did not use cues inside the pool, we rotated the pool daily and removed floating debris and feces before every trial. **Transfer trials:** On transfer trials the mice were placed onto the edge of the pool and allowed to swim with no platform present. The video system recorded the percentage of time spent in the various quadrants. The experimenter recorded from a video monitor the number of times the mouse crossed the previous position of the platform; crosses were defined by the head fully entering the square representing the platform position. **Transfer trial in the absence of visual cues:** To hide distal visual cues, we hung white curtains from the ceiling in a circle (2 m diameter around the pool).

31. A. Baude *et al.*, *Neuroscience* **69**, 1031 (1995); M. E. Rubio and R. J. Wenthold, *Neuron* **18**, 939 (1997).
32. R. A. Silver *et al.*, *J. Physiol. (London)* **493**, 167 (1996).
33. R. C. Malenka and R. A. Nicoll, *Neuron* **19**, 473 (1997).
34. We studied LTP in the lateral and medial perforant path synapses of dentate granule cells. In adult GluR-A<sup>-/-</sup> mice, the magnitude of LTP was about half that of wild type. In wild-type mice ( $n = 4$ ) the values ( $\pm$ SEM) were  $128\% \pm 11\%$  ( $n = 10$ ) and  $132\% \pm 7\%$  ( $n = 8$ ) of the pretetanic amplitudes for the lateral and medial perforant path synapses, whereas GluR-A<sup>-/-</sup> mice ( $n = 5$ ) showed  $113\% \pm 4\%$  ( $n = 10$ ) and  $118\% \pm 5\%$  ( $n = 11$ ) for the same two inputs. The data are not explained by a smaller proportion of mutant slices showing potentiation.
35. N. Meiri *et al.*, *Proc. Natl. Acad. Sci. U.S.A.* **95**, 15037 (1998); S. Schurmans *et al.*, *ibid.* **94**, 10415 (1997); M. Nosten-Bertrand *et al.*, *Nature* **379**, 826 (1996); Y. Y. Huang *et al.*, *Cell* **83**, 1211 (1995); S. Okabe *et al.*, *J. Neurosci.* **18**, 4177 (1998).
36. R. G. M. Morris and U. Frey, *Philos. Trans. R. Soc. London Ser. B* **352**, 1489 (1998).
37. M. Köhler, H.-C. Kornau, P. H. Seeburg, *J. Biol. Chem.* **269**, 17367 (1994).
38. D. Feldmeyer *et al.*, *Nature Neurosci.* **2**, 57 (1999).
39. A. Nagy, J. Rossant, R. Nagy, W. Abramow-Newerly, J. C. Roder, *Proc. Natl. Acad. Sci. U.S.A.* **90**, 8424 (1993).
40. H. Gu, Y.-R. Zou, K. Rajewsky, *Cell* **73**, 1155 (1993).
41. H. Markram *et al.*, *J. Physiol. (London)* **500**, 409 (1997).
42. W. Sather, S. Dieudonne, J. F. MacDonald, P. Ascher, *ibid.* **450**, 643 (1992).
43. P. Jonas, G. Major, B. Sakmann, *ibid.* **472**, 615 (1993).
44. R. Sprengel *et al.*, *Cell* **92**, 279 (1998).
45. K. D. Phend, R. J. Weinberg, A. Rustioni, *J. Histochem. Cytochem.* **40**, 1011 (1992).
46. M. Frotscher, *Microsc. Res. Tech.* **23**, 306 (1992).
47. F. Helmchen, K. Imoto, B. Sakmann, *Biophys. J.* **70**, 1069 (1996).
48. G. Grynkiwicz, M. Poenie, R. Y. Tsien, *J. Biol. Chem.* **260**, 3440 (1985).
49. W. Denk, J. H. Strickler, W. W. Webb, *Science* **248**, 73 (1990); H. J. Koester and B. Sakmann, *Proc. Natl. Acad. Sci. U.S.A.* **95**, 9596 (1998).
50. D. W. Saffin *et al.*, *Proc. Natl. Acad. Sci. U.S.A.* **85**, 7795 (1998).
51. P. H. Kelly and J. Malanowski, *Can. J. Physiol. Pharmacol.* **71**, 352 (1993).
52. K. Kask *et al.*, *Proc. Natl. Acad. Sci. U.S.A.* **95**, 13777

(1998). Membrane proteins of hippocampi were processed for immunoblot analysis with glutamate receptor 1 polyclonal antibody (Chemicon, Temecula, CA) at 0.5 to 1  $\mu\text{g/ml}$ . After visualization by enhanced chemiluminescence (ECL, Amersham Corp.) blots were stripped and reprobed with glutamate receptor 2 polyclonal antibody at 1  $\mu\text{g/ml}$  (T62-3B) (18) and with an NR1 monoclonal antibody (54.1) at 3  $\mu\text{g/ml}$ .

53. Supported in part by the Volkswagen-Stiftung (R.S.,

P.H.S., B.S.), the Deutsche Forschungsgemeinschaft (P.H.S.), and Bristol-Myers Squibb (P.H.S.). We thank H. Gu for the plasmid pMC-Cre, A. Nagy for the R1 ES cell line, R. Morrison and J. R. Wenthold for providing antibodies, and M. Lang, A. Herold, S. Nestel, and B. Joch for technical assistance. D.Z. was the recipient of a postdoctoral fellowship from the Human Frontier Science Program.

3 March 1999; accepted 11 May 1999

## Rapid Spine Delivery and Redistribution of AMPA Receptors After Synaptic NMDA Receptor Activation

Song-Hai Shi,<sup>1</sup> Yasunori Hayashi,<sup>1</sup> Ronald S. Petralia,<sup>2</sup> Shahid H. Zaman,<sup>1</sup> Robert J. Wenthold,<sup>2</sup> Karel Svoboda,<sup>1</sup> Roberto Malinow<sup>1</sup> \*

To monitor changes in  $\alpha$ -amino-3-hydroxy-5-methyl-4-isoxazole propionate (AMPA) receptor distribution in living neurons, the AMPA receptor subunit GluR1 was tagged with green fluorescent protein (GFP). This protein (GluR1-GFP) was functional and was transiently expressed in hippocampal CA1 neurons. In dendrites visualized with two-photon laser scanning microscopy or electron microscopy, most of the GluR1-GFP was intracellular, mimicking endogenous GluR1 distribution. Tetanic synaptic stimulation induced a rapid delivery of tagged receptors into dendritic spines as well as clusters in dendrites. These postsynaptic trafficking events required synaptic *N*-methyl-D-aspartate (NMDA) receptor activation and may contribute to the enhanced AMPA receptor-mediated transmission observed during long-term potentiation and activity-dependent synaptic maturation.

Excitatory synaptic transmission in the vertebrate central nervous system is mediated by activation of AMPA- and NMDA-type glutamate receptors. Repetitive synaptic activity transiently activates NMDA receptors and triggers long-lasting plasticity (1), expressed, at least in part, as an increase in AMPA receptor function (2, 3). The molecular basis for activity-induced changes in AMPA receptor function is not known and may include changes in channel conductance (4), possibly after receptor phosphorylation (5), or delivery of AMPA receptors to synapses, as has been documented during development (6). We investigated if an increase in AMPA receptor number at synapses may occur rapidly during NMDA receptor-dependent synaptic plasticity.

AMPA receptors are oligomers formed by a combination of four different subunits,

GluR1 to 4 (GluR A to D) (7). A substantial proportion of endogenous AMPA receptors in hippocampal neurons have the GluR1 subunit (8). We constructed a recombinant GluR1 tagged with green fluorescent protein (GFP) at the putative extracellular NH<sub>2</sub>-terminus (GluR1-GFP; Fig. 1A) (9). This protein was expressed in human embryonic kidney (HEK) 293 cells; extracts showed a single band by protein immunoblotting of the expected molecular mass (Fig. 1B). Whole-cell recordings from GluR1-GFP-transfected HEK 293 cells showed inwardly rectifying responses to puffed agonist (Fig. 1C) (7). Cotransfection of GluR1-GFP with wild-type GluR2 yielded responses with no rectification (Fig. 1C), indicating effective hetero-oligomerization between GluR1-GFP and GluR2, as homomeric GluR2 can produce little current (7).

GluR1-GFP was introduced into neurons with Sindbis virus expression system (10, 11). In hippocampal dissociated cultured neurons (Fig. 2) (12), GluR1-GFP showed distribution throughout the dendritic tree with expression levels in dendrites approximately three times that of endogenous GluR1 (13). Immunostaining for surface (Fig. 2D) (14)

<sup>1</sup>Cold Spring Harbor Laboratory, Cold Spring Harbor, NY 11724, USA. <sup>2</sup>Laboratory of Neurochemistry, National Institute on Deafness and Other Communication Disorders, National Institutes of Health, Bethesda, MD 20892-4162, USA.

\*To whom correspondence should be addressed. E-mail: malinow@cshl.org